Comparative Analysis of Heat Sink Pressure Drop Using Different Methodologies

C.K. Loh, D.J. Chou
Enertron Inc.
100 W. Hoover Suite 5
Mesa, Arizona 85210
(480) 649-5400
ckloh@enerton-inc.com

Abstract

Pressure drop across heat sink is one of the key variables that govern the thermal performance of the heat sink in forced convection environment. There are several analytical methods to estimate the heat sink pressure drop, however correctly selecting one that can represent the reality over a range of airflow found in typical electronics cooling application is difficult. In this paper, we propose a modified analytical method to estimate the channel velocity and used it to calculate the total heat sink pressure drop through different theoretical pressure drop equations. The theoretical results produced from the theoretical equations were compared against results gathered from experimental study and numerical method.

Keywords

Pressure Drop, Theoretical, Experimental and Numerical.

Nomenclature

A_f	Total free area that allows air flow to pass through, m^2
A_{tf}	Total heat sink frontal area including the base, m^2
b	Width of the heat sink gap, m
D_h	Hydraulic diameter, m
f	Fully developed laminar flow friction factor
f_{app}	Apparent friction
H	Height of the fin, m
K_c	Coefficient of contraction
K_e	Coefficient of expansion
L	Total length of the fin, m
N	Number of fins
ΔP	Heat sink pressure drop, Pa
Re_{ch}	Channel Reynolds Number
t_f	Fin thickness, m
x^+	Hydrodynamic entry length, m
V_{ch}	Heat sink channel velocity, m/s
V_{ap}	Heat sink approach velocity, m/s
W	Total width of the heat sink, m
ρ	Air density, kg/m^3
α	Geometric fraction used in equation (11)
β	Geometric fraction used in equations (9) & (12)
λ	Geometric fraction used in equation (13)
ν	Fluid dynamic viscosity, m^2/s

Introduction

In general, the total heat sink pressure drop depends on four major factors: the friction factors, the heat sink geometry, the approach velocity and the heat sink channel velocity. The friction factors arise from the airflow entering and exiting heat sink channel are known as the contraction loss coefficient and expansion loss coefficient respectively, whereas the friction factor that due to the transition of airflow from developing flow to fully developed flow is called the apparent friction. The expansion and contraction loss coefficient can be determined by heat sink geometry alone, however calculating the apparent friction required not only the heat sink geometry but also the heat sink channel velocity. For this reason, estimating the channel velocity from the approach velocity is critical to obtain a theoretical pressure drop that represents the true heat sink pressure drop. In this paper, the conventional channel velocity equation is replaced with new form of channel velocity equation that takes into consideration the ratio between the sum of each individual channel frontal area and the total frontal heat sink area. The channel velocities computed from the conventional approach and the new equation were then used to compute the total heat sink pressure drop through different pressure drop correlations found in the fluid mechanic literatures and texts. In order to prove the validity of the theoretical pressure drop calculation, four heat sinks with different geometry are put into the wind tunnel for pressure drop experiment. Numerical analysis of these heat sinks was performed using FLOTHERM v4.1 to compare with theoretical and experimental findings.

Theoretical Approach

Three commonly used theoretical equations to solve heat sink pressure drop are listed below. Equation 1 and 2 can be derived from classical Flemings and Darcy pressure drop equations, while Equation 3 can be obtained by considering a force balance on the heat sink.

$$\Delta P = \left(\frac{f_{app} N(2HL + bL)}{HW} + K_c + K_e \right) \left(\frac{1}{2} \rho V_{ch}^2 \right) [1] \qquad (1)$$

$$\Delta P = (4 f_{app} x^+ + K_c + K_e) \left(\frac{1}{2} \rho V_{ch}^2 \right) [2] \qquad (2)$$

$$\Delta P = 4(f_{app} x^{+} + K_c + K_e)\left(\frac{1}{2}\rho V_{ch}^2\right) [3] \quad (3)$$

The coefficients of losses are directly related to the geometry of the heat sink and the hydrodynamic loss is related to the heat sink channel velocity, V_{ch}. When air passes through the heat sink channels, it accelerates and the channel velocity is estimated through the scaling of approach velocity, V_{ap} with a scaled factor. The scale factor (typically the ratio of the heat sink fin geometry) is one of the key parameters to get a more accurate theoretical pressure drop that correlates to the experimental findings. In the conventional approach, the channel velocity is predicted using the approach velocity and the scale factor between heat sink channel width, b and the fin thickness, t_f. It is represented as [4]:

$$V_{ch} = V_{ap}\left(1 + \frac{t_f}{b}\right) \quad (4)$$

To improve the accuracy of the channel velocity prediction, equation (4) is modified and reintroduced in the following form:

$$V_{ch} = V_{ap}\left(\frac{A_f}{A_{tf}}\right) \quad (5)$$

As shown in Figure 1, equation (5) takes into the consideration of the entire heat sink frontal area, A_{tf} and the sum of the frontal heat sink channels area, A_f.

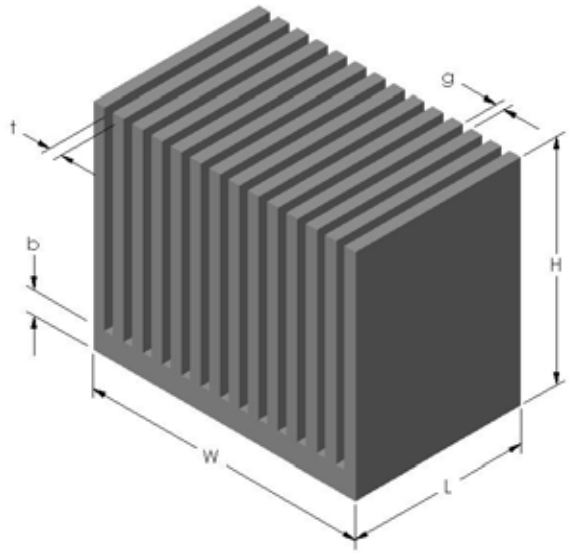

Figure 1 Schematic of heat sink test sample.

The hydrodynamic developing flow apparent friction, f_{app}, is related to hydrodynamic entrance length, x^+, and the fully developed laminar flow friction factor, f, [5]:

$$f_{app}\mathrm{Re}_{ch} = \left[\left(\frac{3.44}{\sqrt{x^+}}\right)^2 + \left(f\mathrm{Re}_{ch}\right)^2\right]^{\frac{1}{2}} \quad (6)$$

Where

$$x^+ = \frac{L}{D_h \mathrm{Re}_{ch}} \quad (7)$$

and the channel Reynolds Number, Re_{ch}, is given by

$$\mathrm{Re}_{ch} = \frac{V_{ch} D_h}{\nu} \quad (8)$$

The fully developed laminar flow friction factor, *f*, can be obtained through a chart published by Kays and London [1] or computed from the following:

$$f\mathrm{Re}_{ch} = 24 - 32.53\beta + 46.72\beta^2 - 40.83\beta^3 + 22.96\beta^4 - 6.09\beta^5 \quad (9)$$

where

$$\beta = \frac{b}{H} \quad (10)$$

The contraction loss coefficient, K_c and the expansion loss coefficient, K_e, for the airflow entering and exiting the heat sink rectangular channels are expressed as:

For equation (1):
$K_c=0.42(1-\alpha^2)$ $K_e=(1-\alpha^2)^2$ (11)

For equation (2):
$K_c=0.8-0.4\lambda^2$ $K_e=(1-\lambda)^2-0.4\lambda^2$ (12)

For equation (3):
$K_c=0.8+0.04\beta-0.44\beta^2$ $K_e=(1-\beta)^2-0.4\beta^2$ (13)

Where

$$\alpha = 1 - \frac{Nt_f}{W} [6] \quad (14)$$

$$\lambda = \frac{b}{(b + t_f)} [1] \quad (16)$$

$$\beta = \frac{b}{H} [2] \quad (15)$$

Experimental Method

Four heat sinks with different geometry were tested in a controlled wind tunnel environment in order to verify the theoretical pressure drop results calculated from the equation (1), (2) and (3). These heat sinks were chosen to cover a broad range of geometry that can provide a good comparison for the calculated theoretical results. The actual images of these heat sinks are shown in Figure 2 and their corresponding dimensions and manufactured types are listed in Table 1. Figure 3 represents the test section of the wind tunnel. The test section measured 150 mm in width, 150 mm in height and 1300 mm in length. The heat sink test sample is place 900 mm down stream measured from the test section inlet. The heat sink is fully ducted on the top and both sides to prevent any bypass. Airflow velocity through the test section is measured by Pitot tube placed approximately 240 mm upstream from the test sample. At the center of the bottom wall where the test sample is located, 8 evenly space pressure taps at 40 mm apart from each other were used to measure pressure drop across the heat sink with different geometry. The heat sinks were subjected to incremental approach velocity in the range of 1 m/s to 5.5 m/s in the ducted channel respectively.

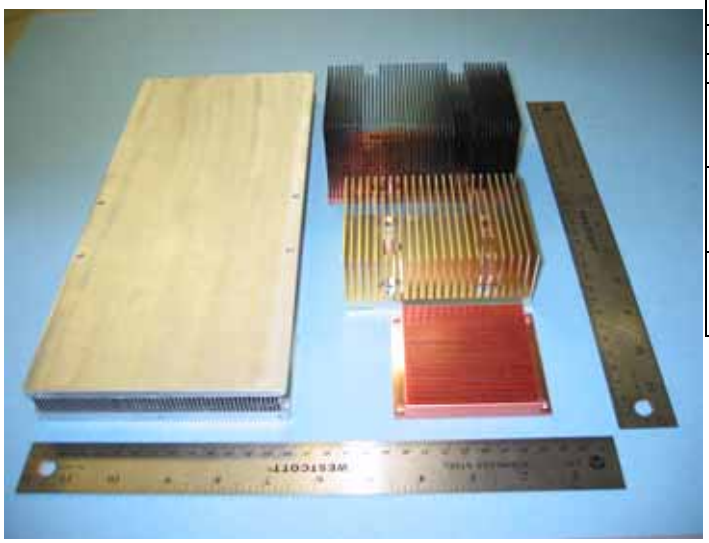

Figure 2 Heat Sinks used for experiment.

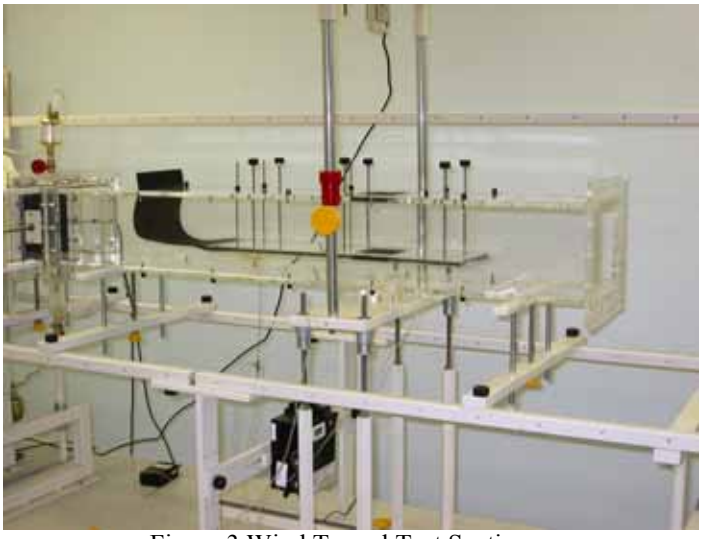

Figure 3 Wind Tunnel Test Section

Table 1. Heat Sink Test Sample Specifications

Test Sample #	1 (Al - Low Profile Extended Length Heat Sink)	2 (Cu - Low Profile Saw Cut Heat Sink)	3 (Cu Base – Solder Bonded Al Fins Heat Sink)	4 (Al – Extruded Heat Sink)
Width (W)	140 mm	69 mm	126 mm	110 mm
Length (L)	350 mm	83 mm	75 mm	75 mm
Height (H)	27 mm	11 mm	63 mm	39 mm
Fin Thickness (t)	0.4 mm	0.65 mm	1 mm	1 mm
Channel Width (g)	2 mm	1.2mm	1.55 mm	4 mm
Base Thickness (b)	12 mm	3.6 mm	7mm	8 mm

Numerical Models

The numerical model for test sample 1, 2, 3 and 4 are shown in Figure 4, 5, 6 and 7 respectively. FLOTHERM v4.1 is used to perform the numerical simulation.

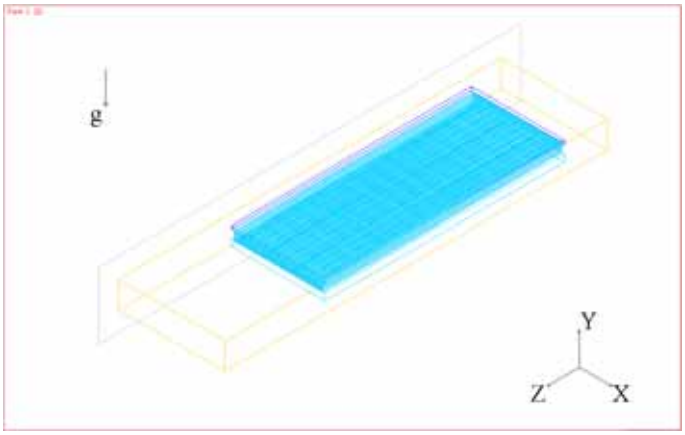

Figure 4. Numerical Model of Test Sample 1

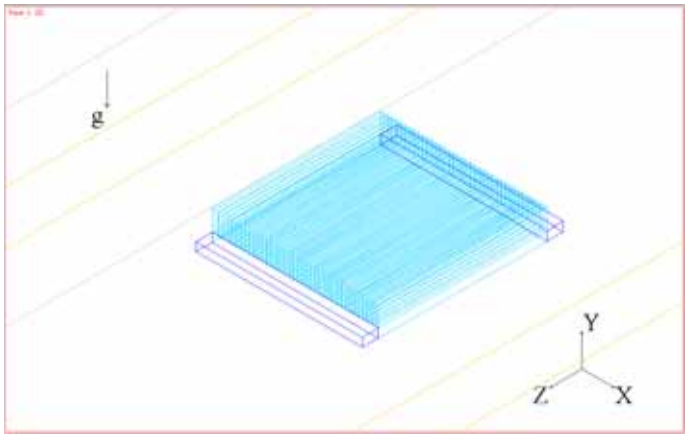

Figure 5. Numerical Model of Test Sample 2

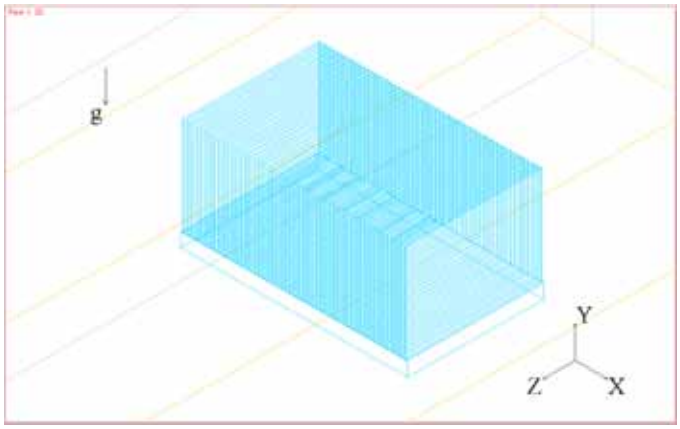

Figure 6. Numerical Model of Test Sample 3

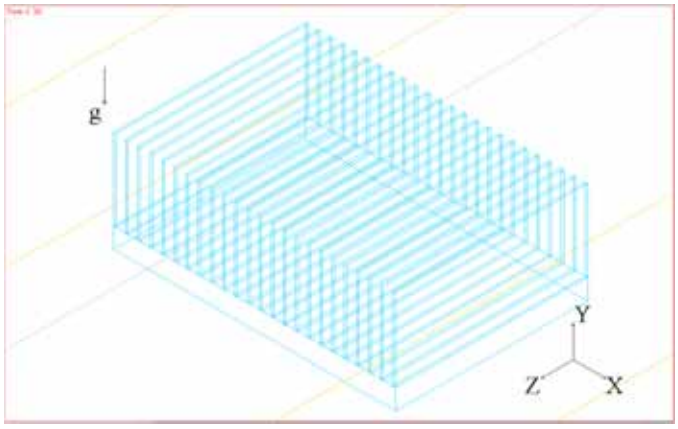

Figure 7. Numerical Model of Test Sample 4

The computational domain for the test sample is presented in Figure 8. The computational domain is model after the ducted section of the wind tunnel test section and for each test sample simulation, the model test section is resizes accordingly. The airflow in the model was generated at the location corresponding to the Pitot tube location in the test section by using the fixed flow option. This option allowed user to construct the flow cross-section area, specify normal velocity or volume flow rate, and air properties evaluated at a specified temperature. The Rectangular cuboids feature in the FLOTHERM was used to form the walls of the wind tunnel and also the ducting plates of the heat sink. The triangular blocks were used to simulate the reduction of cross sectional area in the test section where the heat sink ducted area begins. Monitor points representing the pressure taps are placed in the front and the back of the heat sink to measure the pressure drop across the heat sink. In addition, the monitor points are placed along the ducted area to measure the heat sink approach velocity.

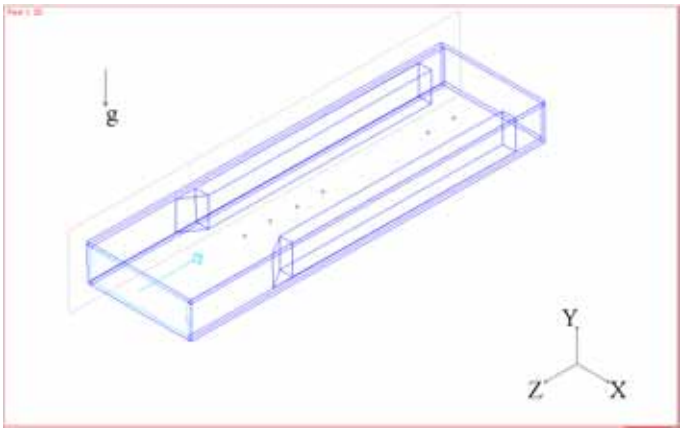

Figure 8. Test Sample Computational Domain

The flow for every test case is considered to be laminar since the Reynolds number is less than 2400 for approach velocity ranges between 1.016 m/s and 5.08 m/s. The air properties attached to the computational domain are evaluated at 30°C. High density logarithm grids are applied to the entrance and exit of the heat sink models to obtain the pressure drop results with higher accuracy. The numbers of computational grid cells used in the 4 different simulations are represented in Table 2.

Table 2. Number of Grid Cells for each Test Sample

	Number of Grid Cells		
	x-direction	*y*-direction	*z*-direction
Test Sample 1	166	16	208
Test Sample 2	124	17	48
Test Sample 3	161	15	52
Test Sample 4	80	16	51

Results

Channel Velocity obtained from Equation (4)

The heat sink pressure drop obtained from experimental, FLOTHERM simulation, equation (1), equation (2) and equation (3) are shown in Figure 8, 9, 10 and 11. The channel velocity used to compute the total heat sink pressure drop in equation (1), (2) and (3) is calculated using equation (4). As shown in the figures, the experimental results and FLOTHERM numerical results are in agreement with each other, however the theoretical equations did not agree with both experimental results and FLOTHERM numerical results. In addition, the figures also illustrated that the theoretical equations under predict the heat sink drop. Among the three

theoretical equations, equation (1) results seem closer to the experimental findings compared against equation (2) and (3).

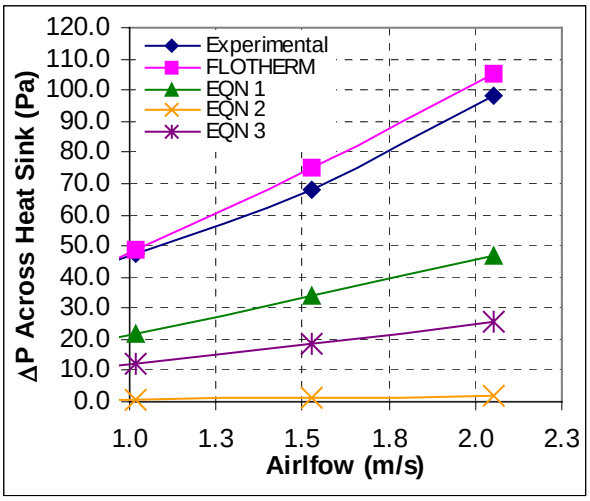

Figure 8. Test Sample 1 ΔP Results

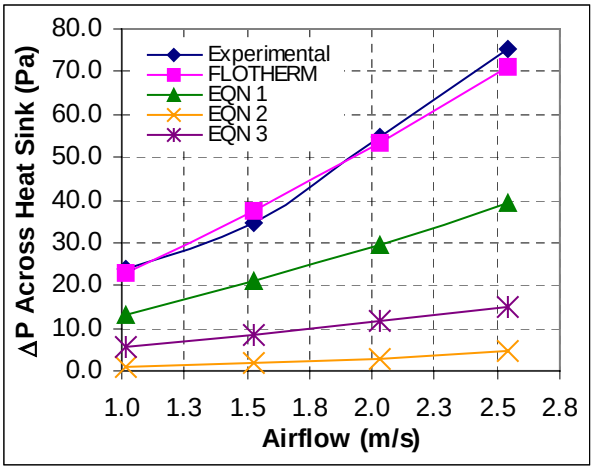

Figure 9. Test Sample 2 ΔP Results

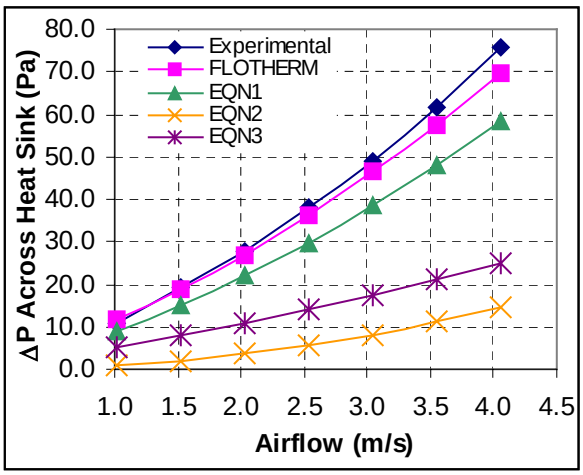

Figure 10. Test Sample 3 ΔP Results

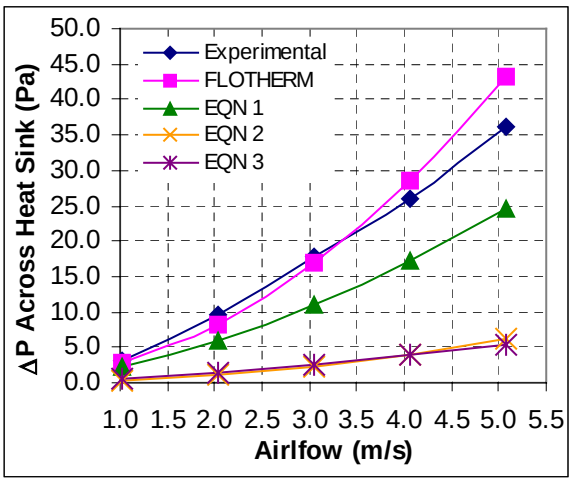

Figure 11. Test Sample 4 ΔP Results

Channel Velocity obtained from Equation (5)

Figure 12, 13, 14 and 15 shows the experimental findings, FLOTHERM numerical results and the theoretical heat sink pressure drops calculated using equation (5). By comparing through all the figures, pressure drop results computed from equation (2) and equation (3) still disagree with the experimental findings, however, equation (1) seems to yield results that closely followed the experimental findings and the FLOTHERM numerical results.

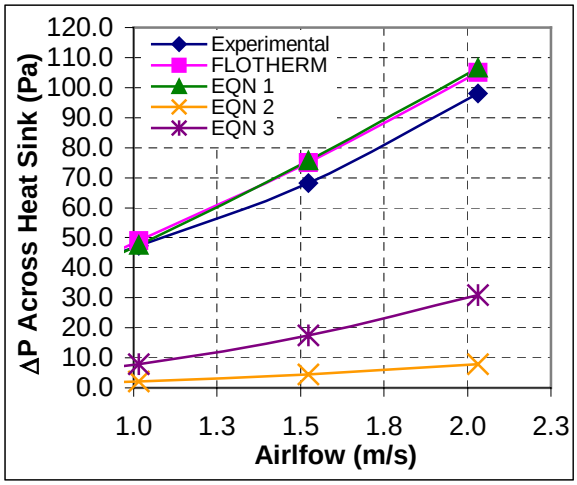

Figure 12. Test Sample 1 ΔP Results

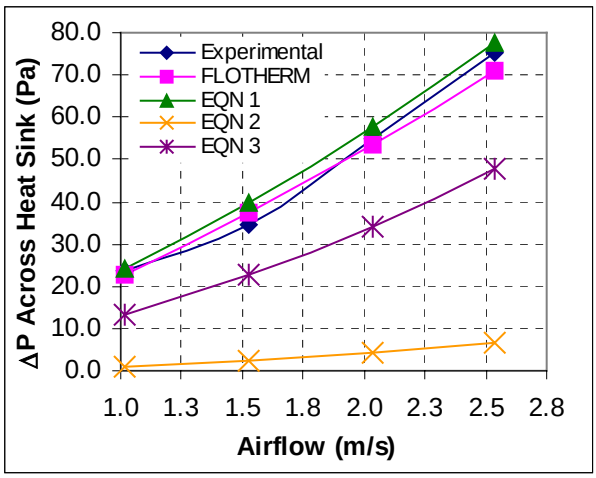

Figure 13. Test Sample 2 ΔP Results

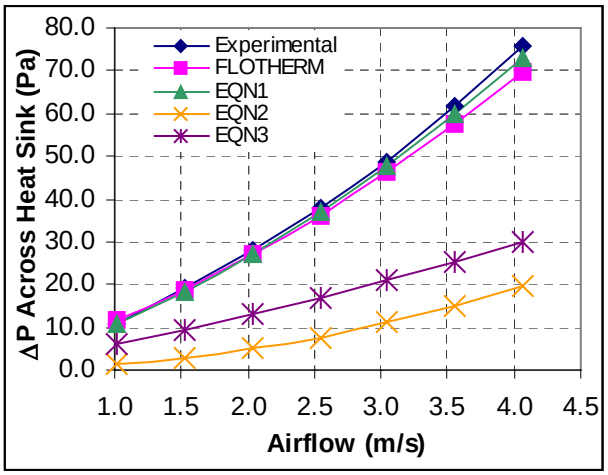

Figure 14. Test Sample 3 ΔP Results

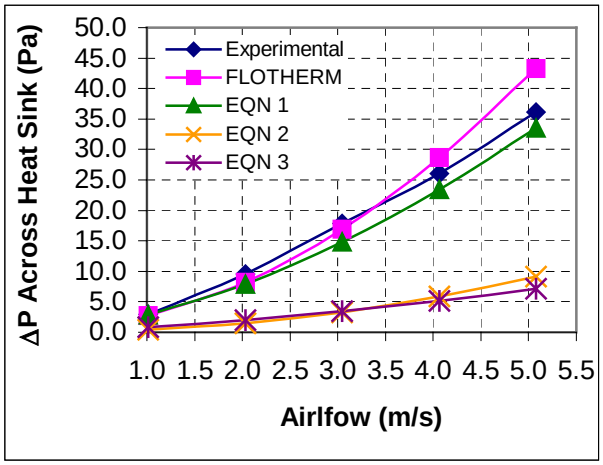

Figure 15. Test Sample 4 ΔP Results

Summary

In short, the pressure drop results found in Results section can be summarized as follow:

- The combination of equation (5) and equation (1) can be used to calculate the theoretical heat sink pressure drop.
- Numerical simulation tools can also served as useful tool to predict the pressure drop.

Despite their poor correlation in predicting the pressure drop compared to equation (1), equation (2) and (3) are by no mean invalid, it means that both equations might not be suitable to produce good results under certain constraints and conditions.

Reference

[1] W. M. Kays and A. L. London, *Compact Heat Exchangers*, 3rd Edition, McGraw-Hill, 1984.

[2] D. Copeland, Optimization of Parallel Plate Heatsinks for Forced Convection, *Proceedings of the 16th IEEE SEMI-THERM Symposium*, pp. 266-272, 2000.

[3] B. R. Munson, D. F. Young and T. H. Okiishi, Fundamentals Of Fluid Mechanics, 2nd Edition, John Wiley & Sons, 1994.

[4] J. R. Culham and Y. S. Muzychka, Optimization Of Plate Fin Heat Sinks Using Entropy Generation Minimizaton, *ITherm 2000*, Volume II, pp. 8-15, 2000.

[5] Y.S., Muzychka and M.M., Yovanovich, "Modelling Friction Factors in Non-Circular Ducts for developing Laminar Flow", *AIAA 98-2492, 2nd AIAA Theoretical Fluid Mechanics Meeting*, Albuquerque, N.M., 1998.

[6] F.M., White, *Fluid Mechanics*, McGraw-Hill, New York, 1987.